Heterogeneity in lung macrophage control of *Mycobacterium tuberculosis* is determined by T cells

Short title: T cell containment of Mtb growth

Rocky Lai, Travis Williams, Tasfia Rakib, Jinhee Lee, and Samuel M. Behar*

Department of Microbiology and Physiological Systems, University of Massachusetts Medical School, Worcester, Massachusetts, USA.

*Correspondence:

Samuel M. Behar

E-mail address: samuel.behar@umassmed.edu

Abstract

Following *Mycobacterium tuberculosis* infection, alveolar macrophages are initially infected but ineffectively restrict bacterial replication. The distribution of *M. tuberculosis* among different cell types in the lung changes with the onset of T cell immunity when the dominant infected cellular niche shifts from alveolar to monocyte-derived macrophages (MDM). We hypothesize that changes in bacterial distribution among different cell types is driven by differences in T cell recognition of infected cells and their subsequent activation of antimicrobial effector mechanisms. We show that CD4 and CD8 T cells efficiently eliminate *M. tuberculosis* infection in alveolar macrophages, but they have less impact on suppressing infection in MDM, which may be a bacterial niche. Importantly, CD4 T cell responses enhance MDM recruitment to the lung. Thus, the outcome of infection depends on the interaction between the T cell subset and the infected cell; both contribute to the resolution and persistence of the infection.

Introduction

Mycobacterium tuberculosis causes the chronic lung infection tuberculosis (TB). Following inhalation of *M. tuberculosis*, alveolar macrophages are initially infected, setting in motion a series of events that result in the recruitment of numerous cell types to the lung, including both innate (e.g., neutrophils and macrophages) and adaptive (e.g., B and T cells) immune cells [1, 2, 3]. These cells cooperate to form granulomas, the characteristic pathological lesion of TB. The fate of granulomas is varied. Some undergo fibrosis and/or calcification. In others, progressive bacterial replication leads to dissemination, necrosis, and cavitation. While most people develop immunity and avoid symptomatic disease, 10% develop clinical TB at some point during their lives. Impairment of cell mediated immunity greatly increases the risk of developing active TB, and genetic, environmental, and microbial factors play a role. Understanding how *M. tuberculosis* is contained is an important question as a major clinical goal is to develop vaccines that prevent susceptible people from developing disease. A better understanding of the mechanisms that lead to containment of infection and why they fail in susceptible individuals is needed.

Tremendous heterogeneity exists among cells in the myeloid lineage. Monocytes, macrophages, dendritic cells (DC), and polymorphonuclear cells (PMNs) (hereafter referred collectively to as “myeloid cells”) both reside in and are recruited to the lung parenchyma during *M. tuberculosis* infection. Heterogeneity is based on cell ontology but is also shaped by homeostatic signals specific for the tissue niches where the cells reside (e.g., alveolar macrophages), and by episodic inflammatory signals that lead to cell recruitment, activation, and differentiation. After inhalation of aerosols containing *M. tuberculosis*, alveolar macrophages (AM) are the first cell type in the lung infected [1]. Subsequently, AM in the alveoli traffic into the parenchyma and trigger innate inflammatory responses. Monocytes and neutrophils are recruited to the lung. Monocytes differentiate into macrophages and dendritic cells [4, 5], which *M. tuberculosis* infects [1, 6, 7, 8, 9]. New experimental approaches show that pre-existing heterogeneity among human macrophages affect *M. tuberculosis* growth [10]. Importantly, macrophages differ in

their intrinsic control of *M. tuberculosis* in vivo, which may be triggered by cell-specific responses [11, 12, 13]. In particular, AM have a metabolic environment that is conducive to bacillary growth by serving as a source of iron and fatty acids, while glycolytically-biased monocyte-derived macrophages (MDM) are more restrictive [11, 12, 14]. While AM are the initial cell type infected after aerosol *M. tuberculosis* infection [1, 12], after infection is established, the number of infected $CD11c^+$ monocyte-derived cells (hereafter, MDM) outnumbers infected AM [1, 9]. While intrinsic features of infected myeloid cells in the lung may affect their propensity to sustain or restrict *M. tuberculosis* growth early after infection, we hypothesize that once adaptive immunity is initiated and recruited to the lungs, T cell immunity will modify the capacity of myeloid cells to restrict *M. tuberculosis* replication.

In animal models, *M. tuberculosis* is controlled within weeks after infection and bacterial exponential growth is replaced by a plateau phase. The timing of this transition is coincident with the development of T cell immunity. The use of $MHCII^{+/+}$/$MHCII^{-/-}$ mixed bone-marrow chimeric mice provides direct evidence that cognate interactions between CD4 T cells and infected cells is important for containment of infection in vivo, although Mtb was not eliminated from $MHCII^+$ lung macrophages [15]. Infected $CD11c^+$ MDM are highly activated, express NOS2, and upregulate CD14, CD38 and ABCA1, to a greater degree than their uninfected counterparts, providing additional evidence that infected cells interact with T cells [9]. Yet, it is paradoxical that MDM should be a dominant reservoir of *M. tuberculosis* and show evidence of being activated by T cells. These data suggest that T cell control of Mtb-infected macrophages is suboptimal and raises the possibility of a cellular niche that supports continued bacillary persistence.

Not all *M. tuberculosis*-specific T cells efficiently recognize *M. tuberculosis*-infected macrophages, depending on the antigen [16, 17] and the number of bacilli per macrophage [18, 19, 20, 21]. It is unknown whether the interaction of CD4 and CD8 T cells with *M. tuberculosis*-infected cells varies depending on the type of infected cell. We hypothesize that some *M. tuberculosis* bacilli occupies a protected cellular niche. We reasoned that for cell types in which *M. tuberculosis*

could be eliminated or its growth restricted by T cells, T cell depletion would lead to an increase in infected cells. In contrast, for cell types in which *M. tuberculosis* persists, even in the face of T cell pressure, T cell depletion should have minimal effect. We report that CD4 and CD8 T cells cooperate to restrict *M. tuberculosis* infection in several types of infected cells. *M. tuberculosis*-infection in AM is efficiently controlled by T cells, particularly by CD4 T cells. In contrast, both CD4 and CD8 T cells are required to restrict *M. tuberculosis* replication in MDM. Interestingly, T cell depletion had the least effect on MDM compared to other cell types. This hierarchy is the reverse of the intrinsic capacity of AM and MDM to control bacterial replication early after infection. Thus, depending on the cell type, the influence of T cells on *M. tuberculosis* containment varies. We propose that although T cell interact with *M. tuberculosis*-infected MDM, they have a limited ability to restrict infection in these cells. Although MDM are better than AM in their intrinsic capacity to restrict intracellular *M. tuberculosis*, once T cell immunity is initiated, AM largely inhibit *M. tuberculosis* growth while T cells contribute only modestly to the ability of MDM to limit intracellular infection.

Results

CD4 and CD8 T cells synergize to restrict *M. tuberculosis* growth in the lung.

To determine how T cells exert pressure on different types of *M. tuberculosis*-infected macrophages, we combined low dose aerosol infection with Rv.YFP [9] and antibody-mediated depletion of T cells. The in vivo infection was allowed to progress for three weeks, during which time T cell immunity to *M. tuberculosis* is initiated and recruited to the lung [2, 3]. Then, groups of mice were treated with a control antibody, antibody to CD4, to CD8, or a combination of anti-CD4 and anti-CD8 for two weeks. The mice were analyzed 5 weeks post infection (wpi) (Fig.1a). Both CD4 and CD8 T cells were eliminated from the lungs of *M. tuberculosis* infected mice, although CD8 depletion was slightly less efficient (Fig.1b). Neither CD4 nor CD8 T cell depletion led to a statistically significant increase in lung CFU (Fig.1c). In contrast, the combined depletion of CD4 and CD8 T cells led to an increase in lung CFU (Fig.1c). These data show that early after infection, both CD4 and CD8 T cells make a synergistic contribution to controlling *M. tuberculosis* replication in vivo.

Monocyte-derived macrophages are the dominant cellular niche for *M. tuberculosis*.

Advances in multiparametric flow cytometry have improved our ability to characterize myeloid cells in the lung. We adapted our myeloid flow panel for spectral flow cytometry and measured the distribution of *M. tuberculosis* among different myeloid cell types in the lung, 3- and 5-weeks post-infection. Some important technical features of the panel and its analysis are described in the *Methods*. Myeloid cells were defined as live $CD45^+$ cells after lymphoid cells were excluded based on the CD19, Thy1.2, and NK1.1 lineage markers. Neutrophils and eosinophils were identified by their expression of Ly6G and SiglecF, respectively (Figure 2a). CD64 and Mertk distinguished macrophages from non-macrophages (i.e., monocytes and DC).

Alveolar macrophages (AM) were discriminated from other lung macrophages by their high levels of SiglecF and CD11c. CD11b expression divided AM into two subsets. Non-AM

120 macrophages have been called recruited macrophages (RM), interstitial macrophages (IM) and
121 CD11c^{Hi} monocyte-derived cells (MDC) [5, 9, 11, 12]. We previously referred to these cells as CD11c^{Hi};
122 however, in recognition of heterogeneity in their CD11c expression, we have dropped the CD11c
123 moniker. As these monocyte-derived cells are distinct from resident macrophages (e.g., AM), we
124 refer to them as monocyte-derived macrophages (MDM). MDM were divided into three subsets
125 based on their SiglecF and CD11c expression. The SiglecF^{int}CD11c^{+} (MDM1) were the most
126 variable between experiments and could be immature AM [22, 23, 24]. SiglecF^{-}CD11c^{+} (MDM2) were
127 the most abundant of the three and were most like what we previously referred to as CD11c^{Hi}
128 MDC (Figure 2a) [9]. In additions, SiglecF^{-}CD11c^{-} (MDM3) may be nerve associated macrophages
129 that have been recently described in the lung [25]. Finally, we subdivided monocytes and DC (M/DC)
130 based on CD11c and Ly6C expression (M/DC1-4). The most abundant of these were M/DC1
131 (Ly6c^{-}CD11c^{VAR}) and M/DC3 (Ly6c^{+}CD11c^{-}). The former was likely a mixed DC population, and
132 the latter were probably classical monocytes.

133 Between three and five weeks after infection, the total number of macrophages and
134 monocyte/DCs in the lung significantly increased (Figure S1a). During this interval, the number of
135 *M. tuberculosis*-infected macrophages increased 5.4-fold, while the number of infected
136 eosinophils, neutrophils, and monocyte/DCs remained the same. This led to macrophages
137 becoming the dominant infected cell type (Figure S1b, S1c). With the greater granularity afforded
138 by spectral flow cytometry, we defined what was driving these changes in 11 predefined cell
139 subsets (Figure 2a). Between three and five weeks after infection, SiglecF^{-}CD11c^{+} non-AM
140 macrophages (i.e., MDM2) underwent a 14-fold increase in cell number such that they accounted
141 for ~14% of the lung myeloid cells (Figure 2b). M/DC1 cells (Ly6c^{-}CD11c^{+}), also increased in
142 number (Figure 2b). Thus, the dominant myeloid cell types in the lung changed from
143 predominantly neutrophils and monocytes (M/DC3) to macrophages (MDM2) and DC (M/DC1).
144 This was accompanied by a dramatic shift in the type of cells infected by *M. tuberculosis* (Figure
145 2c). The number of *M. tuberculosis*-infected non-alveolar macrophages (MDM1, -2, -3) all

146 increased by more than 10-fold. In absolute numbers, MDM2 increased the most and came to
147 account for 45% of infected cells (Figure 2c). To confirm that these results were not due to
148 differences in YFP expression between the different macrophage populations, we determined the
149 intracellular CFU within AM and MDM from the lungs of infected B6 mice. Consistent with our
150 flow cytometric analysis (Figure 2a, c), MDM had 10-fold more *M. tuberculosis* CFU than AM
151 (Figure 2d). The significant increase in *M. tuberculosis*-infected macrophage number occurred
152 despite the onset of T cell immunity during this phase of infection [26, 27]. We hypothesized that
153 MDM could represent a cellular niche against which T cell immunity inefficiently controlled *M.*
154 *tuberculosis* replication.
155
156 **The effectiveness of T cell immunity depends on the type of infected cell.**
157 We predicted that a cellular niche that was shielded from T cell immunity would be largely
158 unaffected by T cell depletion, compared to cell types that require T cell signals to restrict
159 intracellular *M. tuberculosis* replication. As described above, three weeks after infection, once
160 effector T cells were recruited to the lung, groups of mice were treated with mAb to CD4, CD8 or
161 both CD4 and CD8 for two weeks. Then, the frequency of *M. tuberculosis*-infected cells was
162 determined for 11 myeloid cell types by flow cytometry (Figure 1a, 2a).
163 T cell depletion led to a statistically significant increase in the percentage of infected
164 neutrophils, AM1, MDM1, and MDM2 (Figure 3a, b). Only combined CD4 and CD8 depletion led
165 to an increased frequency of *M. tuberculosis*-infected neutrophils, suggesting that CD4 and CD8
166 T cells are redundant in their ability to control infection in these cells (Figure 3b). In contrast, CD4
167 depletion alone led to a significantly increased frequency of infected AM1, MDM1, and MDM2
168 (Figure 3a, b). Although CD8 depletion alone had no effect, CD4 and CD8 double depletion
169 significantly increased the frequency of infected AM1, MDM1, and MDM2 compared to CD4
170 depletion alone (Figure 3a, b). Importantly, these data indicate CD4 and CD8 T cells act
171 synergistically to control *M. tuberculosis* infection in macrophages in vivo. Only depletion of CD4

and CD8 T cells led to an increase in the number of bacilli per cell in AM1, AM2, and MDM1, based on the median fluorescence intensity of Rv.YFP (Figure 3c). Interestingly, the Rv.YFP signal of MDM2, the most abundant infected cell type, was unaffected by T cell depletion (Figure 3c).

We next analyzed how T cell pressure affected the frequency of infected cells among all myeloid cells, since the abundance of each cell type varies. In control (undepleted) mice, MDM2 made the largest contribution (Figure 3d). CD4 T cell significantly augmented the fraction of infected neutrophils and AM1 among myeloid cells (Figure 3b, 3d). In contrast, CD4 T cell depletion did not alter the contribution of infected MDM2. While CD8 depletion alone had no effect, combined anti-CD4 and anti-CD8 mAb treatment significantly increased the frequency of infected neutrophils and M/DC2, compared to anti-CD4 or CD8 mAb treatment alone. Combined CD4 and CD8 depletion also increased the fraction of infected MDM1 and MDM2. However, the contribution of MDM2 to *M. tuberculosis*-infected myeloid cells after CD4+CD8 depletion increased 1.4-fold (compared to undepleted mice). This change was small compared to the increased proportion of infected neutrophils or AM1 (9.5- and 5.8-fold, respectively). Thus, even though MDM are highly activated, their high rate of infection and dominant niche for *M. tuberculosis* raise the possibility that they are inefficiently recognized by T cells [16, 18, 28]. Conversely, the emergence of other cell populations as an important niche for *M. tuberculosis* after T cell depletion shows that T cell immunity effectively controls *M. tuberculosis* infection in other myeloid cell types.

CD4 T cells maintain high levels of NOS2 expression by macrophages.

Nitric oxide synthase 2 (NOS2) is induced by IFNγ in macrophages and its expression is essential for survival of mice after *M. tuberculosis* infection. NOS2 converts L-arginine into nitric oxide (NO), which is toxic to *M. tuberculosis*; however, its role in vivo is more complicated as is its relevance to human TB [29]. NOS2 is expressed by *M. tuberculosis*-infected macrophages in the

lung lesions of B6 mice, both by AM and MDM [9, 12, 30]. We measured NOS2 expression by myeloid cells in the lung following *M. tuberculosis* infection and T cell depletion as described above. At baseline (i.e., undepleted), 25-42% of MDM1 and MDM2 expressed NOS2 (Figure 4a). Other cell types such as AM1, MDM3, and M/DC2 also produced significant amounts of NOS2. The NOS2 expression by these different cell types correlated with their degree of infection (Figure 4b, r=0.98). In general, more cells in each population expressed NOS2 than were infected. This led us to determine how many *M. tuberculosis*-infected cells expressed NOS2 (Figure 4c). There were too few eosinophils and AM2 to generate reliable data. However, for the other subsets, there was a hierarchy of NOS2 producing cells. Nearly 100% of the *M. tuberculosis*-infected MDM subsets expressed NOS2. In contrast, ~70% of AM1, 50-60% of M/DC except for M/DC3 produced NOS2. We did not detect intracellular NOS2 in neutrophils (Figure 4c).

We next looked at the effect of T cells on the expression of NOS2 in *M. tuberculosis*-infected cells by segregating the frequency of $NOS2^+$ vs. $NOS2^-$ infected cells. After CD4 depletion, slightly more than half of the *M. tuberculosis*-infected cells failed to express NOS2. CD4 depletion led to an increase in *M. tuberculosis*-infected neutrophils and AM1, and most infected cells failed to express NOS2 (Figure 4d). Consistent with our previous results, CD8 depletion did not affect the frequency of *M. tuberculosis*-infected cells nor their expression of NOS2, although it modestly increased the number of infected neutrophils. The ratio of $NOS2^+$ vs. $NOS2^-$ infected cells was decreased after CD4 and CD4+CD8 depletion in all myeloid populations (Figure 4d, e). Remarkably, although ~50% of the *M. tuberculosis*-infected MDM2 no longer expressed NOS2 after CD4 or CD4/CD8 depletion, the frequency of infected cells only increased incrementally (Figure 4d). Interestingly, the ratio of $NOS2^+/NOS2^-$ infected cells was increased in AMs after CD8 depletion but not in MDM (Figure 4d, e). Although NOS2 continues to be expressed in myeloid cells even in the absence of T cells, these data indicate that CD4 T cells are crucial for maintaining high levels of NOS2 expression in infected macrophages.

Aminoguanidine treatment does not affect control of *M. tuberculosis* infection.

NOS2 is essential for resistance to *M. tuberculosis* infection in B6 mice and mice that lack the NOS2 gene succumb to infection 4-5 wpi [31]. NO has been suggested to be more important in regulating inflammation than in direct killing of *M. tuberculosis* [32, 33]. We tested whether inhibition of NOS2 in vivo, through administration of aminoguanidine (AG), would exacerbate *M. tuberculosis* infection as observed with CD4 T cell depletion. To verify that AG treatment was successful, NO was measured in lung homogenate using the Griess reaction. AG appeared to have successfully inhibited the production of NO by NOS2 (data not shown). We observed an increase in the number of viable bacilli in the lungs but not the spleens of mice treated with AG for two weeks (Figure 5a, 5b). The total number of neutrophils and M/DC3 but not any of the other myeloid populations were significantly increased after treatment (Figure 5c). The frequency of infected neutrophils was increased after AG treatment, consistent with the exacerbation of TB disease as previous described [33]. However, AG treatment did not alter the proportion of infected cells among the other myeloid subsets (Figure 5d). Thus, it appears that this early stage of *M. tuberculosis* infection after T cell recruitment to the lung, NO has little or no role in the control of *M. tuberculosis* within macrophage subsets.

CD4 T cells drive the recruitment of MDM to the site of infection.

Our data suggests that AM depend on CD4 T cells to augment their intrinsic capacity to control *M. tuberculosis* (Figure 3a). In contrast, MDMs are less sensitive to the loss of T cell pressure. T cells secrete numerous chemokines including CCL2, CCL3, and CCL4, which direct cellular recruitment to the site of infection. As such, we postulated that CD4 T cells recruitment of myeloid cells to the lung could augment containment of *M. tuberculosis* infection. could recruit MDM to the lung. To determine whether T cells were important in the recruitment of myeloid cells, C57BL/6 and $RAG^{-/-}$ mice, the latter being devoid of B and T cells, were infected with *M. tuberculosis*. At 3 weeks post infection, CD4 T cells from infected C57BL/6 mouse were

transferred via the intravenous route to the $RAG^{-/-}$ mice (Figure 6a). As expected, transfer CD4 T cells were sufficient to protect help contain *M. tuberculosis* (Figure 6b). *M. tuberculosis* infection of $RAG^{-/-}$ mice led to an increase in many of the different myeloid cell types in the lung (Figure 6c). Transfer of immune polyclonal CD4 T cells led to a large significant increase in the number of MDM in the lung (Figure 6c). Immune polyclonal CD4 T cells reduced the fraction of *M. tuberculosis* infected cells (Figure 6d, left) and decreased the intracellular bacillary load, based on YFP MFI (Figure 6d, right), for most of the myeloid cell types in the lung. Given these effects of CD4 T cells, one would expect that the total number of *M. tuberculosis* infected cells should decrease. Although one sees dramatic reductions in the number of infected AM and neutrophils, the number of infected MDM and other cells did not significantly change (Figure 6e, left). In fact, because of these changes, CD4 T cells induce a shift in the dominant infected cell type from neutrophils to MDM (Figure 6e, right).

Discussion

The interaction between T cells and infected phagocytes determines the course of *M. tuberculosis* infection. While T cell immunity is required to contain infection, it is not sufficient to sterilize mice or the approximately 10% of people that develop active tuberculosis. In the murine TB literature, infection of pulmonary DC has been reported, but using better lineage markers, multiparametric flow cytometry, and single cell RNASeq, it now appears that $CD11c^+$ macrophages are the dominant infected macrophage population in the lung [9, 11, 12]. Given the inherent diversity of cell types, activation states, and degree of infection of cells in the lung, we asked whether the impact of T cell immunity is equally distributed among different myeloid cell types. We hypothesized that there could exist cellular niches in which *M. tuberculosis* is able to persist because T cells are unable to recognize certain infected cells. Here we report that T cell control of intracellular infection depends on the type of infected cell. *M. tuberculosis*-infection of AM is efficiently limited by T cells. In contrast, T cells have only a modest impact on controlling *M. tuberculosis*-infection among MDM.

Using a newly designed flow antibody panel that takes advantage of spectral flow cytometers, we validated our previous results and those of other labs. Three weeks after low dose aerosol *M. tuberculosis* infection, most bacilli are found within three cell populations: neutrophils, macrophages, and monocyte/DCs. By five weeks, relatively few bacteria reside in DC or monocytes; instead, most *M. tuberculosis* is within macrophages. The macrophages are of two types: AM and MDM. With additional markers, the macrophages can be subdivided into 5 populations. A priori, these different macrophage populations could reflect different ontogeny or activation states. For example, significantly more $CD11b^+$ AM were infected than $CD11b^-$ AM. As CD11b is upregulated upon AM activation [9, 11, 12], we speculate that uninfected $CD11b^-$ AM could occupy uninfected regions of the lung. Similarly, we find that the expression of SiglecF and CD11c among the MDM defined three distinct populations and responded differently to *M. tuberculosis* infection.

CD8 depletion had little or no effect on early *M. tuberculosis* recrudescence in the lung. Similarly, CD4 depletion led to a statistically significant increase in only one of three experiments. In contrast, dual depletion led to a dramatic increase in *M. tuberculosis* burden in the lung. The increase in lung and spleen CFU tracked with the distribution of Rv.YFP in infected cells. An exact correlation between CFU and YFP^+ should not be expected as flow cytometric analysis cannot assess extracellular Mtb, differentiate between live and dead bacilli, and only poorly assess the number of bacilli/cell. CD4 depletion increased the frequency of YFP^+ neutrophils and macrophages, and the increase of *M. tuberculosis*-infected cells was even greater after dual CD4 and CD8 depletion. The greater perturbation in the distribution of *M. tuberculosis* among myeloid cells following CD4 but not CD8 depletion suggests that CD4 and CD8 T cell effectors are only partially redundant [16, 18]. Alternatively, depletion of CD4 T cells might not be efficiently compensated by CD8 T cells because CD4 T cell help is required to maintain CD8 T cell antibacterial effector function [34]. The large changes in the frequency of infected cells that occurred when both CD4 and CD8 T cells were depleted indicates that CD4 and CD8 T cells have a synergistic role in mediating control of *M. tuberculosis* infection in both AM and MDM subsets.

In addition to the synergistic role of CD4 and CD8 T cells in mediating control of *M. tuberculosis* infection, our data also points to differential requirements for these T cell subsets in helping AM and MDM to contain *M. tuberculosis*. While CD8 T cells appear to have minimal impact on the ability of AM to control intracellular *M. tuberculosis*, CD8 T cells are important in the ability of MDM to restrict *M. tuberculosis* growth. We and others have demonstrated that CD8 T cells are more efficient at recognizing cells with high bacterial burden [20, 21], and the difference in intracellular burden between AM and MDM could explain why the two populations react differently to the loss of CD8 T cell pressure.

NOS2 is essential for host resistance to *M. tuberculosis* infection in B6 mice, and mice that lack the NOS2 gene succumb to infection after 4-5 weeks [31]. Induction of nitric oxide (NO) requires two canonical signals: IFNγ and a microbial signal such as LPS [35]. Nitric oxide (NO)

315 production by NOS2-expressing macrophages can kill *M. tuberculosis in vitro* and has led to the
316 paradigm that IFNγ production by CD4 T cells induces NO production by macrophages, leading
317 to control of *M. tuberculosis* [36]. The *in vivo* role of NO is less certain. NO regulates inflammation
318 during *M. tuberculosis* infection in vivo [33]. We find NOS2 expression by macrophages was
319 diminished only after CD4 depletion. NOS2 expression by macrophages was similar after CD4
320 depletion or dual CD4 and CD8 depletion, indicating that CD8 T cells had no effect on NOS2
321 expression and suggesting that CD8 T cells may not rely on the induction of NOS2 to control *M.*
322 *tuberculosis.*

323 As CD4 depletion led to reduced NOS2 expression and increased frequency of YFP^+
324 macrophages, *in vivo* inhibition of NOS2 should mimic CD4 depletion should lead to a loss of
325 bacterial control. Surprisingly, aminoguanidine treatment of *M. tuberculosis* infected mice had no
326 effect on the intracellular *M. tuberculosis* burden within either AM or MDM, despite evidence of
327 NO inhibition. However, we do observe increased recruitment of neutrophils as well as an
328 increase in overall lung CFU, both of which have been previous reported following treatment with
329 aminoguanidine [33]. One possibility is that the length of the treatment wasn't long enough to
330 significantly perturb the intracellular burden to the point where we can detect intracellular
331 changes. The lack of change on the intracellular *M. tuberculosis* burden following aminoguanidine
332 treatment may also point towards an IFNγ-independent effector mechanism for controlling the
333 growth of intracellular *M. tuberculosis* within AM and MDM [37, 38, 39].

334 The idea that AM ineffectively restricts *M. tuberculosis* is based on their "M2-like" nature
335 and improved host control of pulmonary *M. tuberculosis* after their depletion [40]. David Russell's
336 lab elegantly showed that IM (herein referred to as MDM) have a greater intrinsic ability to control
337 *M. tuberculosis* than AM [12]. Thus, AM appear to be a sanctuary for *M. tuberculosis*. Yet, these
338 data focus on early events after infection. Our data provide additional context for what
339 subsequently happens. Early on, neutrophils, macrophages, and monocytes/DCs are infected
340 similarly. However, once immune T cells are recruited to the lung, monocyte-derived

341 macrophages harbor the bulk of *M. tuberculosis* by five weeks after infection. A caveat of our
342 studies is that they focus on relatively early (i.e., 3-5 wpi) interactions between T cells and lung
343 macrophage subsets. Many studies show that early and late T cell responses differ greatly [41]. It
344 will be important to characterize lung macrophage subsets and their interactions with T cells
345 during chronic infection, although this remains technicially challenging. Still, it is paradoxical that
346 $CD11c^{+}$ MDM are better able to control *M. tuberculosis* infection [12] but are also the major niche
347 for *M. tuberculosis* [9]. Our data shows that the relative permissiveness of macrophage for *M.*
348 *tuberculosis* is modified by T cells. Initially, AM poorly constrain *M. tuberculosis*, but T cells
349 dramatically improve the ability of AM to control intracellular infection. In the absence of T cells,
350 AM emerge again as a haven for *M. tuberculosis*. In contrast, MDM become a niche where *M.*
351 *tuberculosis* persists in the long term even in the presence of T cells.

352 Why would this be the case? We speculate that MDM are already optimally activated
353 following *M. tuberculosis* infection and MDM have an intrinsic capacity to restrict *M. tuberculosis.*
354 While T cells promote MDM control of *M. tuberculosis* infection, the magnitude of this effect is
355 less than for AM. T cells, and T cell factors adds little to the intrinsic ability of MDM to control *M.*
356 *tuberculosis* infection. Over time, their intrinsic activation could potentially impair their APC
357 function if degradation of *M. tuberculosis* antigens prevented reduced their flow into antigen
358 presentation pathways. Alternatively, we consider the possibility that macrophages with only one
359 or two bacteria could be difficult for T cells to recognize. Interestingly, we observed that T cells
360 reduced the bacillary content of infected cells to a point, and the minimum value was similar for
361 all the different cell types. If the intrinsic antibacterial activity of MDM reduces the intracellular
362 bacterial burden without killing the bacilli, the result could be a macrophage where *M. tuberculosis*
363 persists but can't be recognized by T cells. Finally, there is an additional factor. Transfer of CD4
364 T cells to RAG knockout mice leads to reduced CFU and YFP signal compared to un-transferred
365 mice, showing CD4 T cells are critical to protection. However, CD4 T cells also promote the
366 recruitment of macrophages to the lung, presumably through the elaboration of chemokines such

as CCL2, CCL5, or CX3CL1. Although monocyte and macrophage recruitment to an inflammatory site is generally viewed as a beneficial response, in the case of tuberculosis, it provides a new crop of macrophages that can be infected by *M. tuberculosis* and are permissive for its survival and replication.

Methods

Ethics Statement. Studies involving animals were conducted following relevant guidelines and regulations, and the studies were approved by the Institutional Animal Care and Use Committee at the University of Massachusetts Medical School (Animal Welfare A3306-01), using the recommendations from the Guide for the Care and Use of Laboratory Animals of the National Institutes of Health and the Office of Laboratory Animal Welfare.

In vivo infection. C57BL/6J were purchased from Jackson Laboratories (Bar Harbor, ME). H37Rv expressing yellow fluorescent protein (YFP) has been previously described [9, 42]. The mice were exposed to an aerosolized inoculum of Rv.YFP using a Glas-Col Inhalation Exposure System (Glas-Col LLC, Terre Haute, IN) as described [34, 43]. The number of *M. tuberculosis* deposited in the lungs was determined for each experiment and varied ranging between 37–90 CFU.

CD4 and CD8 T cell depletion. 200 µg of either anti-CD4 (clone GK1.5) or anti-CD8 (clone 2.43) mAb were injected intra-peritoneally biweekly starting on day 21 for 14 days to deplete CD4 and/or CD8 T cells.

Lung cell preparation. To isolate total lung leukocytes, lungs were perfused by slowly injecting PBS into right ventricle immediately after mice were killed. The lungs were minced with a gentleMACS dissociator (Miltenyi) and digested (30 min, 37°C) in 250 U/ml collagenase and 60 U/ml DNase (both from Sigma-Aldrich). Lung cell suspensions were passed through a 70-µm and 40-µm strainers sequentially to remove cell clumps. Lung cells were resuspended in autoMACS running buffer (Miltenyi) that contains BSA, EDTA, and 0.09% sodium azide for subsequent staining.

Flow cytometry analysis. Cells were first stained with Zombie Fixable Viability dye (Biolegend) for 10 minutes at room temperature (RT), after which cells were stained with 5 ug/ml of anti-mouse CD16/32 mAb (BioXcell) in autoMACS running buffer (Miltenyi) for 10 minutes at 4°C. Next, the cells were then stained with a surface antibody cocktail for 20 minutes at 4°C. The antibodies included a dump channel was used to exclude T cells, B cells, and NK cells for efficient myeloid cell analysis and included anti-Thy1.2 (clone 30H12), anti-CD19 (clone 6D5), and anti-NK1.1 (clone PK136) with PE-Cy7. Macrophages were subsequently defined based on a combination of CD11c (clone N418), SiglecF (clone E50-2440), Mertk (clone 2B10C42), CD64 (clone X54-5/7.1), Ly6c (clone HK1.4). To inactivate the bacteria, samples were fixed with 1% paraformaldehyde/PBS for 1 hour at room temperature and then washed with MACS buffer. Samples were run on either a 4 or 5 laser Cytek Aurora. Erdman (non-fluorescent) infected mice used for unstained control, single stains and YFP-FMO. Autofluorescence was treated as a fluorescent parameter during unmixing either automatically through the SpectralFlo software or by manually deriving an autofluorescence fingerprint (assigned to BV510). After unmixing FMOs were used to apply manual compensation to correct for unmixing anomalies. Flow data were analyzed using FlowJo v10.7.1.

Adoptive transfer model: Spleens and lymph nodes from C57BL/6J mice were mechanically disrupted onto 70 µm strainers using the plungers of 3 mL syringes. CD4 T cells were purified from spleens and lymph nodes using MojoSort™ CD4 isolation kit and magnet (Biolegend). Purities of cells were determined for each experiment using flow cytometry. 2-5 million CD4 T cells were transferred into TCRα KO mice before infecting with Erdman.

Cell sorting. Cells were sorted using Sony MA900 located in the biosafety level 3 lab in University of Massachusetts Medical School. Cells were stained with Zombie violet to exclude dead cells. Target cells were separated 2-way into polypropylene FACS tubes containing 2 ml of FBS. CD45

(clone 104) was used to identify hematopoietic cells, after which Thy1.2 (clone 30H12), CD19 (clone 6D5) and Ly6G (clone 1A8) were used to remove lymphocytes and neutrophils. Macrophages were identified using a combination of CD11c (clone N418), SiglecF (clone E50-2440), Mertk (clone 2B10C42), CD64 (clone X54-5/7.1).

Aminoguanidine treatment and NO quantification. Mice were supplied with drinking water containing 2.5% aminoguanidine hemisulfate (A7009-100G Sigma) starting from week 3 post infection. Water was replaced once a week. Nitric oxide levels were quantified in lung homogenates using a Greiss assay (G4410-10G Sigma) as previously described [33].

Statistical analysis. Statistical analysis was performed using Prism 9 (GraphPad). P-values were calculated using unpaired t test, one-way ANOVA, or two-way ANOVA as indicated in the figure legends.

Acknowledgements. This work was funded by NIH/NIAID grants to S.M.B.: R01AI106725, R01 AI123286, and P01 AI132130.

Author contribution. Conceptualization, R.L. and S.M.B.; Methodology, R.L., and J.L.; Investigation, R.L., T.W., T.R., and J.L.; Formal analysis, R.L., T.W., and S.M.B.; Writing & Editing, R.L., T.W., T.R., and J.L., and S.M.B.; Supervision, S.M.B.; Funding Acquisition, S.M.B.

Declaration of interests. The authors declare no competing interests.

Figure legends.

Figure 1: The effect of CD4 and CD8 T cell depletion on lung and spleen CFU.

(A) Experimental schematic. Mice were infected with Rv.YFP as indicated and rested for 3 weeks, after which CD4 and CD8 depleting mAbs were given over the course of two weeks at the indicated timepoints. (B) Proportion of CD4 and CD8 T cells in the lungs of infected C57BL/6 mice at 5 weeks post infection following treatment with either anti-CD4 and/or anti-CD8 depleting mAbs. (C) Lung and spleen CFU at 5 weeks post infection following treatment either anti-CD4 and/or anti-CD8 depleting mAbs. Each point represents an individual mouse from two independent experiments (n=5/group) for week 3 data, and three independent experiments for week 5 data. Each condition was compared to the undepleted group using the Brown-Forsythe and Welch's ANOVA test was performed.

Figure 2: Distribution of *M. tuberculosis*-infected cells early after infection.

(A) Gating strategy for identifying various myeloid populations. In brief, a viability dye was used to exclude dead cells. CD3, CD19 and NK1.1 were used to exclude lymphocytes and NK cells from the hematopoietic cells. Mertk and CD64 were used to separate macrophages from monocyte/DC subsets. SiglecF and CD11c were used to separate AM from MDM populations, then used to subset various MDM populations. CD11b was used to subset different AM populations. CD11c and Ly6c were used to subset various monocyte/DC populations. (B) Quantification of various myeloid cells in the lung at week 3 and week 5 post infection, expressed in terms of total cell numbers (top) or as a percentage of total myeloid cells (bottom). (C) Quantification of the YFP signal in various myeloid cells in the lung at week 3 and week 5 post infection, expressed in terms of total cell numbers (top), %YFP of each population (middle) or the fraction of each population of the total YFP+ cells (bottom). (D) Flow sorted AM and MDM2 were plated to determine intracellular CFU within each purified population. (C, D) Each point represents

471 an individual mouse from two independent experiment (n=5/group) for week 3 data, and three
472 independent experiments for week 5 data. A two-way ANOVA was performed using Bonferonni's
473 multiple comparison test. (D) Representative results from two different experiments using cells
474 purified from lung cells pooled from five mice, tested in triplicate, and analyzed using a t-test.
475
476 Figure 3: Lung myeloid cells react differently to the loss of CD4 and CD8 T cell pressures.
477 Quantification of YFP signal within various myeloid populations in the lung at 5 weeks post
478 infection following CD4 and/or CD8 depletion. (A) Representative flow plots of YFP signal in AM1
479 and MDM2, plotted against autofluorescence. Top number represents the frequency of YFP+
480 events, bottom number are the total number of YFP+ cells. (B-D) Graphical representation of YFP
481 signal in different myeloid subsets, expressed as (B) %YFP+ cells within each subset (C) MFI of
482 YFP within each subset (D) and %YFP+ cells out of total myeloid cells. Each point represents an
483 individual mouse from two independent experiments (n=5/group). A two-way ANOVA was
484 performed using Tukey's multiple comparison test. Some statistical comparisons have been
485 omitted for clarity.
486
487 Figure 4: T cell depletion affects NOS2 expression. (A) The percentage of different myeloid cell
488 types in the lung that express NOS2 5 wpi. (B) Correlation between %NOS2 expression and
489 %YFP signal in various myeloid populations. (C) The percentage of infected (YFP+) cells that
490 express NOS2. (D) The effect of CD4 and/or CD8 T cell depletion on the distribution of YFP+ cells
491 among NOS2+ and NOS2– cells, as a percentage of total myeloid cells in the lung 5 wpi. (E) Data
492 from panel D expressed as a ratio of NOS2+ vs. NOS2– cells. Each point represents an individual
493 mouse. The data is representative data from one of two independent experiments (n=5/group). A
494 two-way ANOVA was performed using "Šídák's multiple comparisons test.
495

Figure 5: Inhibition of NOS2 does not increase intracellular bacterial burden. (A) Experimental schematic for AG treatment. Mice were giving AG in their drinking water starting from week 3 post infection over the course of two weeks. (B) Lung and spleen CFU from mice treated with AG at 5 wpi. (C) Total numbers of various myeloid populations in the lung at 5 wpi. (D) %YFP+ as a fraction of total myeloid cells following AG treatment at 5 wpi. Each point represents an individual mouse from two independent experiments (n=5/group). A two-way ANOVA was performed using Tukey's multiple comparison test (D) or Dunnett's test (E).

Figure 6. Adoptive transfer of CD4 T cells drive recruitment of MDM to the lung. (A) Experimental schematic for CD4 T cell adoptive transfer. $RAG^{-/-}$ were infected with Rv.YFP as indicated and rested for 3 weeks. In parallel, C57BL/6 mice were also infected with *M. tuberculosis* Erdman strain, and at 3 wpi, polyclonal CD4 T cells were purified and transferred i.v. into the $RAG^{-/-}$ mice. Cells were isolated from $RAG^{-/-}$ mice two weeks post transfer, and bacterial burden was also examined. (B) Lung CFU was determined in $RAG^{-/-}$ mice that either received CD4 T cells or PBS. (C) Total numbers of various myeloid populations were also enumerated at this timepoint. (D) % YFP (left) and the MFI of YFP (right) within each myeloid population was examined. (E) Total number of YFP+ cells within each myeloid subset (left) and the % of infected cells within each population as a fraction of total infected cells (right). The data is representative data from one of three independent experiments (n=5/group). Statistical analysis was performed using a t-test (B), a two-way ANOVA with Tukey's multiple comparison test (C), or Šídák's multiple comparisons (D, E).

519 **References**
520
521 1. Cohen SB*, et al.* Alveolar Macrophages Provide an Early Mycobacterium tuberculosis Niche and
522 Initiate Dissemination. *Cell Host Microbe* **24**, 439-446 e434 (2018).
523
524 2. Wolf AJ*, et al.* Initiation of the adaptive immune response to Mycobacterium tuberculosis
525 depends on antigen production in the local lymph node, not the lungs. *J Exp Med* **205**, 105-115
526 (2008).
527
528 3. Chackerian AA, Alt JM, Perera TV, Dascher CC, Behar SM. Dissemination of Mycobacterium
529 tuberculosis Is Influenced by Host Factors and Precedes the Initiation of T-Cell Immunity.
530 *Infection and Immunity* **70**, 4501-4509 (2002).
531
532 4. Skold M, Behar SM. Tuberculosis triggers a tissue-dependent program of differentiation and
533 acquisition of effector functions by circulating monocytes. *J Immunol* **181**, 6349-6360 (2008).
534
535 5. Norris BA, Ernst JD. Mononuclear cell dynamics in M. tuberculosis infection provide
536 opportunities for therapeutic intervention. *PLoS Pathog* **14**, e1007154 (2018).
537
538 6. Gonzalez-Juarrero M, Shim TS, Kipnis A, Junqueira-Kipnis AP, Orme IM. Dynamics of macrophage
539 cell populations during murine pulmonary tuberculosis. *J Immunol* **171**, 3128-3135 (2003).
540
541 7. Wolf AJ*, et al.* Mycobacterium tuberculosis infects dendritic cells with high frequency and
542 impairs their function in vivo. *J Immunol* **179**, 2509-2519 (2007).
543
544 8. Repasy T*, et al.* Intracellular bacillary burden reflects a burst size for Mycobacterium
545 tuberculosis in vivo. *PLoS Pathog* **9**, e1003190 (2013).
546
547 9. Lee J, Boyce S, Powers J, Baer C, Sassetti CM, Behar SM. CD11cHi monocyte-derived
548 macrophages are a major cellular compartment infected by Mycobacterium tuberculosis. *PLoS*
549 *Pathog* **16**, e1008621 (2020).
550
551 10. Bryson BD*, et al.* Heterogeneous GM-CSF signaling in macrophages is associated with control of
552 Mycobacterium tuberculosis. *Nat Commun* **10**, 2329 (2019).
553
554 11. Pisu D, Huang L, Grenier JK, Russell DG. Dual RNA-Seq of Mtb-Infected Macrophages In Vivo
555 Reveals Ontologically Distinct Host-Pathogen Interactions. *Cell Rep* **30**, 335-350 e334 (2020).
556

12. Huang L, Nazarova EV, Tan S, Liu Y, Russell DG. Growth of Mycobacterium tuberculosis in vivo segregates with host macrophage metabolism and ontogeny. *J Exp Med*, (2018).

13. Rothchild AC*, et al.* Alveolar macrophages generate a noncanonical NRF2-driven transcriptional response to Mycobacterium tuberculosis in vivo. *Sci Immunol* **4**, (2019).

14. Pisu D*, et al.* Single cell analysis of M. tuberculosis phenotype and macrophage lineages in the infected lung. *J Exp Med* **218**, (2021).

15. Srivastava S, Ernst JD. Cutting edge: Direct recognition of infected cells by CD4 T cells is required for control of intracellular Mycobacterium tuberculosis in vivo. *J Immunol* **191**, 1016-1020 (2013).

16. Yang JD*, et al.* Mycobacterium tuberculosis-specific CD4+ and CD8+ T cells differ in their capacity to recognize infected macrophages. *PLoS Pathog* **14**, e1007060 (2018).

17. Bold TD, Banaei N, Wolf AJ, Ernst JD. Suboptimal activation of antigen-specific CD4+ effector cells enables persistence of M. tuberculosis in vivo. *PLoS Pathog* **7**, e1002063 (2011).

18. Patankar YR*, et al.* Limited recognition of Mycobacterium tuberculosis-infected macrophages by polyclonal CD4 and CD8 T cells from the lungs of infected mice. *Mucosal Immunol* **13**, 140-148 (2020).

19. Sutiwisesak R*, et al.* A natural polymorphism of Mycobacterium tuberculosis in the esxH gene disrupts immunodomination by the TB10.4-specific CD8 T cell response. *PLOS Pathogens* **16**, e1009000 (2020).

20. Lewinsohn DA, Heinzel AS, Gardner JM, Zhu L, Alderson MR, Lewinsohn DM. Mycobacterium tuberculosis-specific CD8+ T cells preferentially recognize heavily infected cells. *Am J Respir Crit Care Med* **168**, 1346-1352 (2003).

21. Mott D, Yang J, Baer C, Papavinasasundaram K, Sassetti CM, Behar SM. High Bacillary Burden and the ESX-1 Type VII Secretion System Promote MHC Class I Presentation by Mycobacterium tuberculosis-Infected Macrophages to CD8 T Cells. *J Immunol* **210**, 1531-1542 (2023).

22. McCubbrey AL, Allison KC, Lee-Sherick AB, Jakubzick CV, Janssen WJ. Promoter Specificity and Efficacy in Conditional and Inducible Transgenic Targeting of Lung Macrophages. *Front Immunol* **8**, 1618 (2017).

23. Aegerter H*, et al.* Influenza-induced monocyte-derived alveolar macrophages confer prolonged antibacterial protection. *Nat Immunol* **21**, 145-157 (2020).

24. Misharin AV*, et al.* Monocyte-derived alveolar macrophages drive lung fibrosis and persist in the lung over the life span. *J Exp Med* **214**, 2387-2404 (2017).

25. Ural BB*, et al.* Identification of a nerve-associated, lung-resident interstitial macrophage subset with distinct localization and immunoregulatory properties. *Sci Immunol* **5**, (2020).

26. Chackerian AA, Alt JM, Perera TV, Dascher CC, Behar SM. Dissemination of Mycobacterium tuberculosis is influenced by host factors and precedes the initiation of T-cell immunity. *Infect Immun* **70**, 4501-4509 (2002).

27. Cooper AM. Cell-Mediated Immune Responses in Tuberculosis. *Annual Review of Immunology* **27**, 393-422 (2009).

28. Lewinsohn DM, Lewinsohn DA. The Missing Link in Correlates of Protective Tuberculosis Immunity: Recognizing the Infected Cell. *Front Immunol* **13**, 869057 (2022).

29. Jamaati H*, et al.* Nitric Oxide in the Pathogenesis and Treatment of Tuberculosis. *Front Microbiol* **8**, 2008 (2017).

30. Mogues T, Goodrich ME, Ryan L, LaCourse R, North RJ. The relative importance of T cell subsets in immunity and immunopathology of airborne Mycobacterium tuberculosis infection in mice. *The Journal of experimental medicine* **193**, 271-280 (2001).

31. MacMicking JD, North RJ, LaCourse R, Mudgett JS, Shah SK, Nathan CF. Identification of nitric oxide synthase as a protective locus against tuberculosis. *Proc Natl Acad Sci U S A* **94**, 5243-5248 (1997).

32. Mishra BB*, et al.* Nitric oxide controls the immunopathology of tuberculosis by inhibiting NLRP3 inflammasome-dependent processing of IL-1beta. *Nat Immunol* **14**, 52-60 (2013).

33. Mishra BB*, et al.* Nitric oxide prevents a pathogen-permissive granulocytic inflammation during tuberculosis. *Nat Microbiol* **2**, 17072 (2017).

34. Lu YJ, Barreira-Silva P, Boyce S, Powers J, Cavallo K, Behar SM. CD4 T cell help prevents CD8 T cell exhaustion and promotes control of Mycobacterium tuberculosis infection. *Cell Rep* **36**, 109696 (2021).

35. Lowenstein CJ*, et al.* Macrophage nitric oxide synthase gene: two upstream regions mediate induction by interferon gamma and lipopolysaccharide. *Proc Natl Acad Sci U S A* **90**, 9730-9734 (1993).

36. Nunes-Alves C, Booty MG, Carpenter SM, Jayaraman P, Rothchild AC, Behar SM. In search of a new paradigm for protective immunity to TB. *Nat Rev Microbiol* **12**, 289-299 (2014).

37. Lu LL*, et al.* IFN-γ-independent immune markers of Mycobacterium tuberculosis exposure. *Nature Medicine* **25**, 977-987 (2019).

38. Van Dis E*, et al.* IFN-gamma-independent control of M. tuberculosis requires CD4 T cell-derived GM-CSF and activation of HIF-1alpha. *PLoS Pathog* **18**, e1010721 (2022).

39. Sakai S*, et al.* CD4 T Cell-Derived IFN-gamma Plays a Minimal Role in Control of Pulmonary Mycobacterium tuberculosis Infection and Must Be Actively Repressed by PD-1 to Prevent Lethal Disease. *PLoS Pathog* **12**, e1005667 (2016).

40. Khan A, Singh VK, Hunter RL, Jagannath C. Macrophage heterogeneity and plasticity in tuberculosis. *J Leukoc Biol* **106**, 275-282 (2019).

41. Jayaraman P*, et al.* TIM3 Mediates T Cell Exhaustion during Mycobacterium tuberculosis Infection. *PLoS Pathog* **12**, e1005490 (2016).

42. Lovewell RR, Baer CE, Mishra BB, Smith CM, Sassetti CM. Granulocytes act as a niche for Mycobacterium tuberculosis growth. *Mucosal Immunol*, (2020).

43. Lai R*, et al.* Host genetic background is a barrier to broadly effective vaccine protection: Relevance to BCG and Mycobacterium tuberculosis Infection. *J Clin Invest* **(in press)**, (2023).

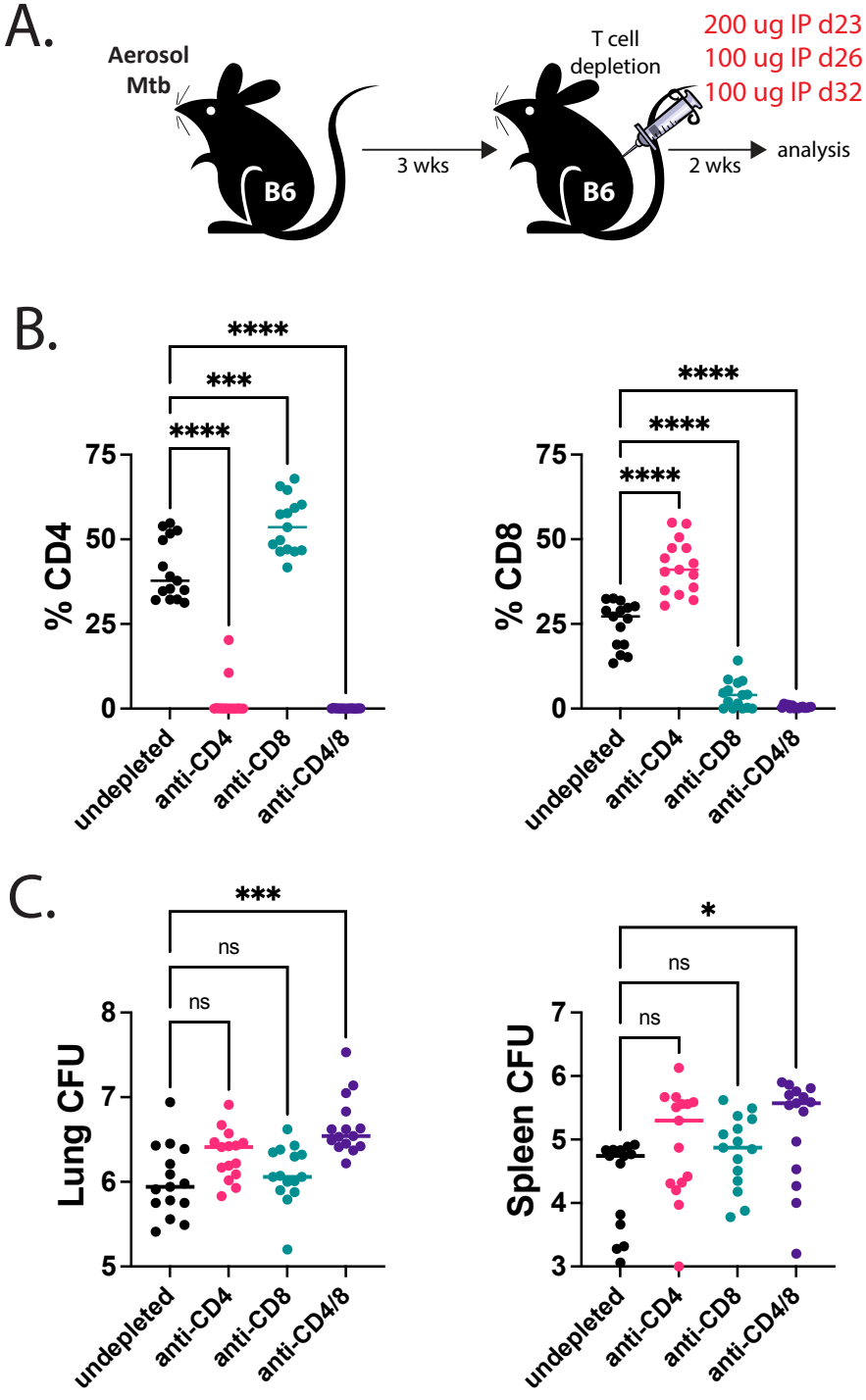

Figure 1

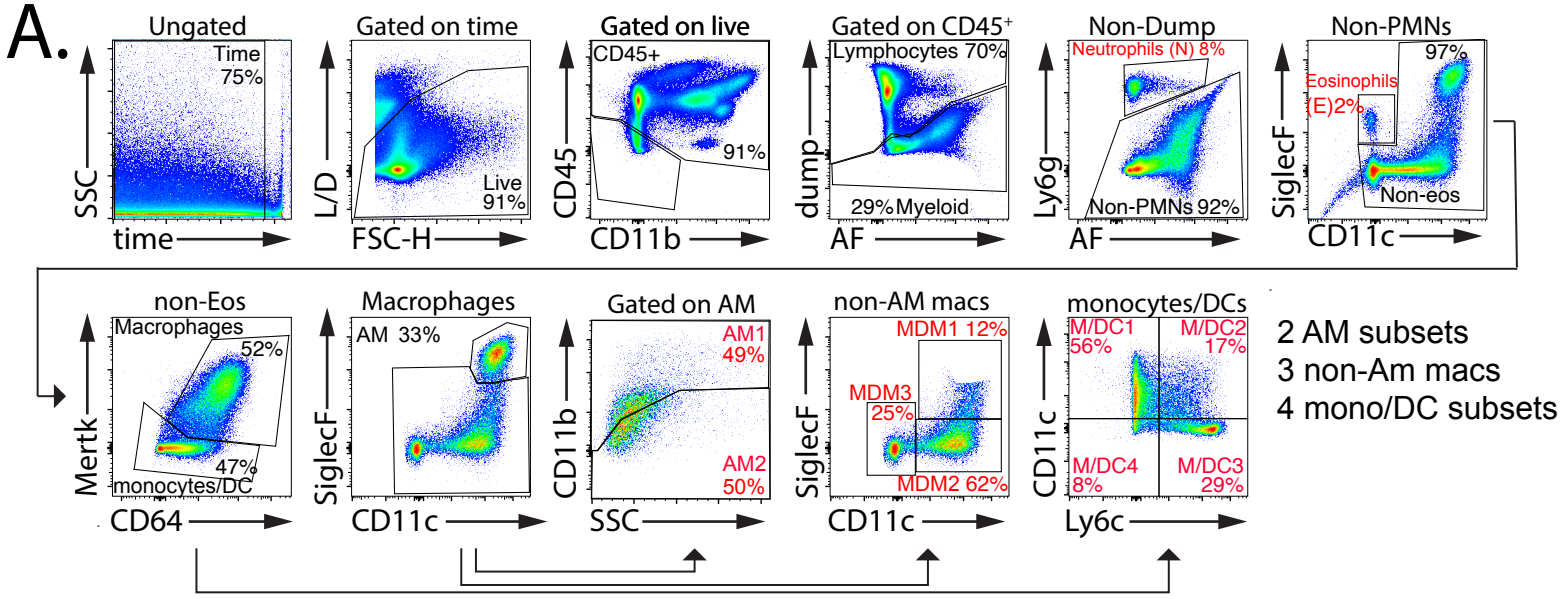

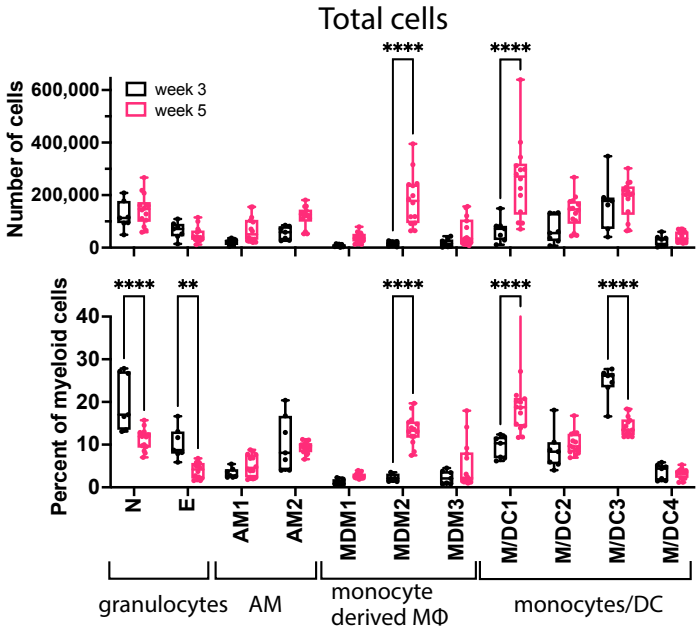

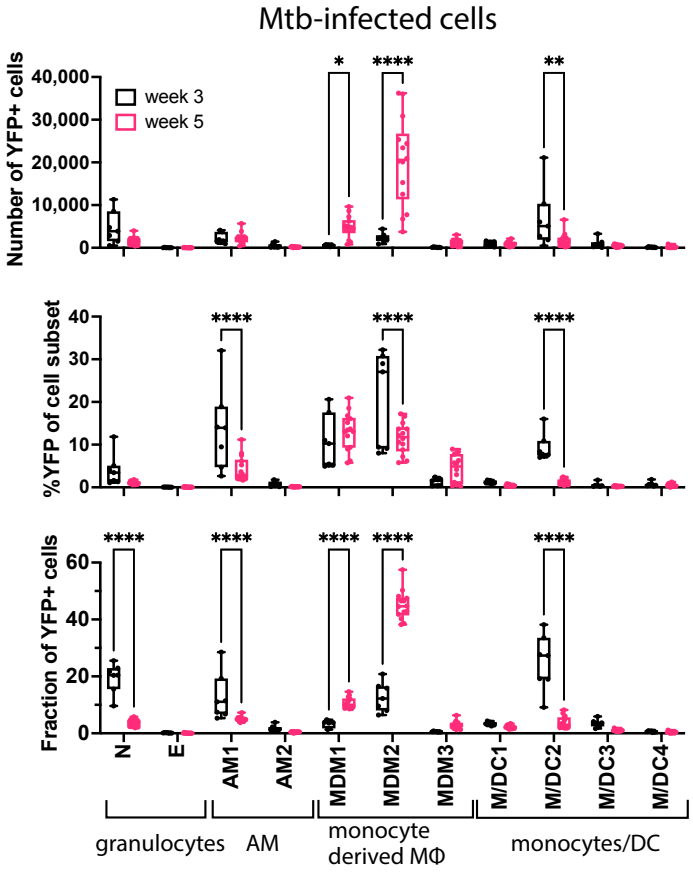

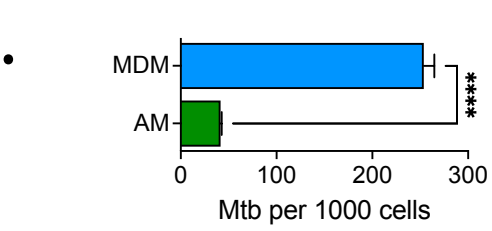

Figure 2

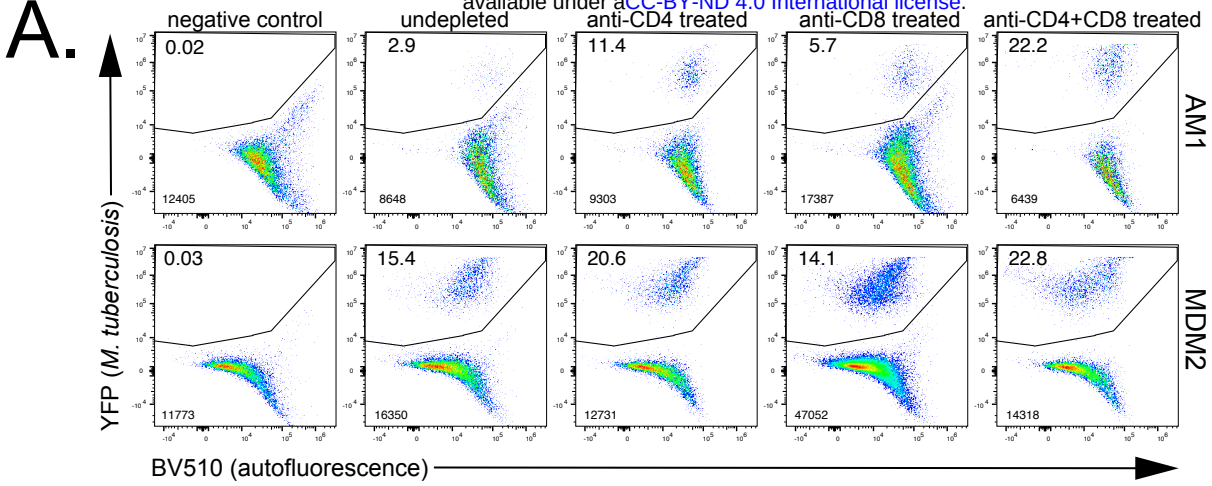

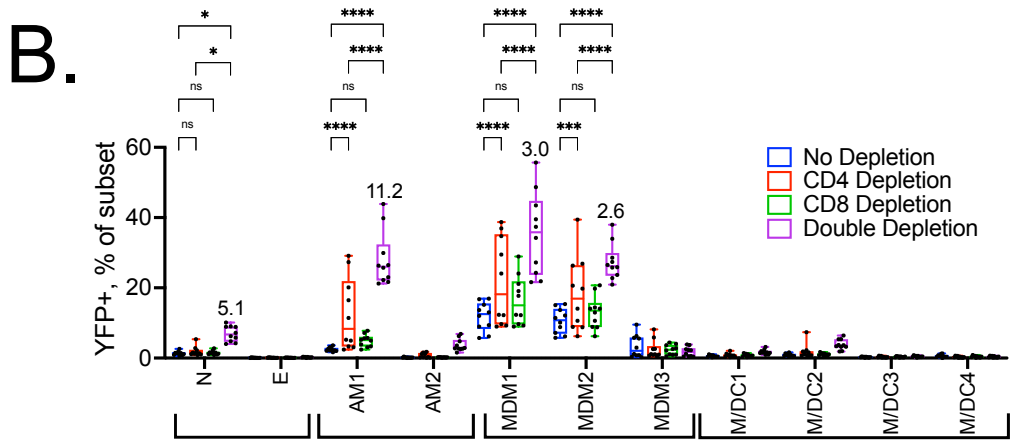

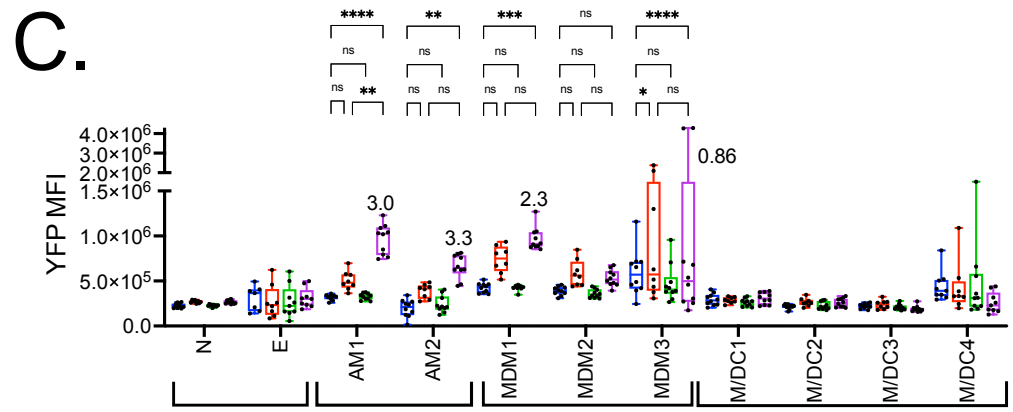

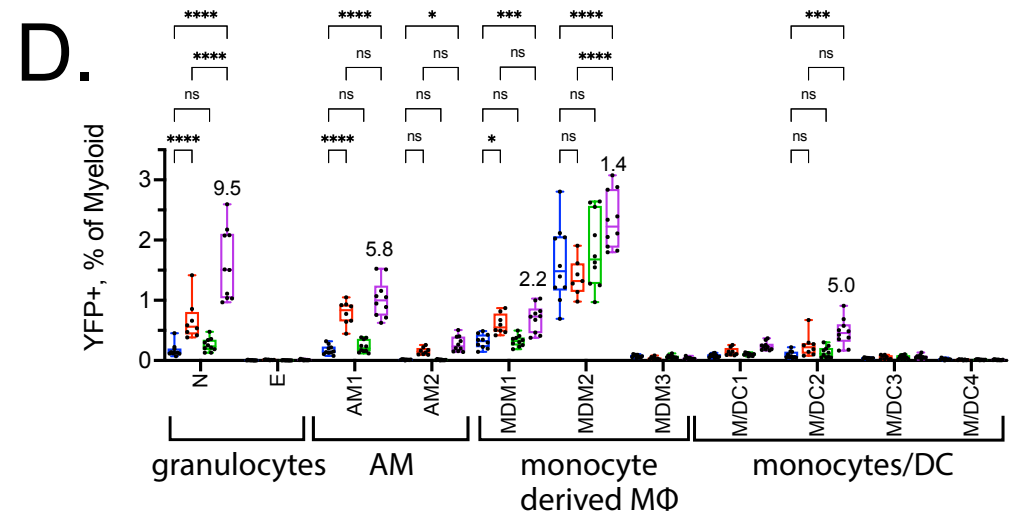

Figure 3

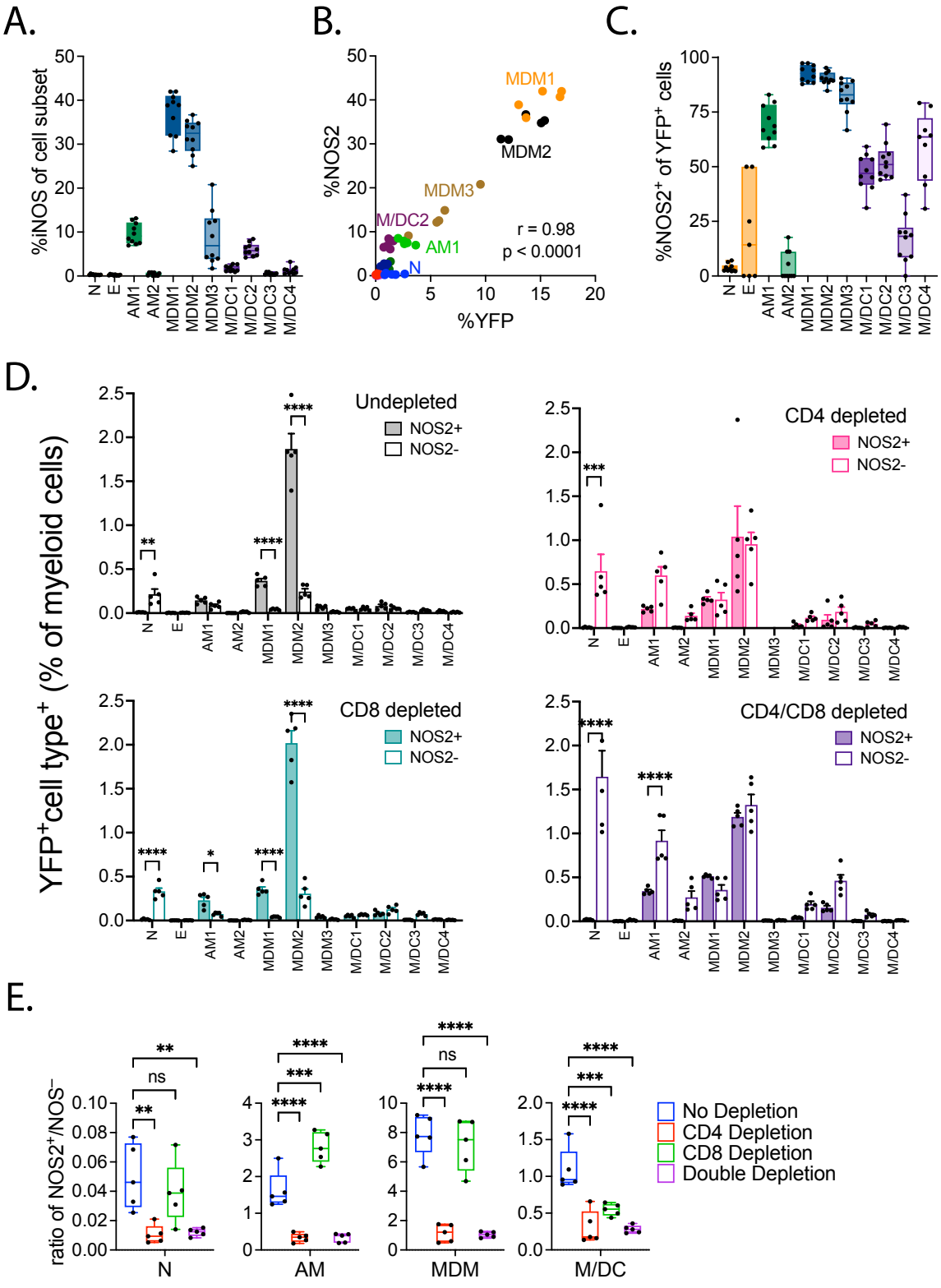

Figure 4

A.

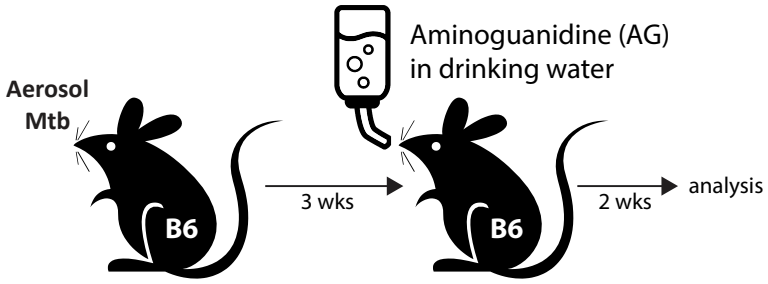

B.

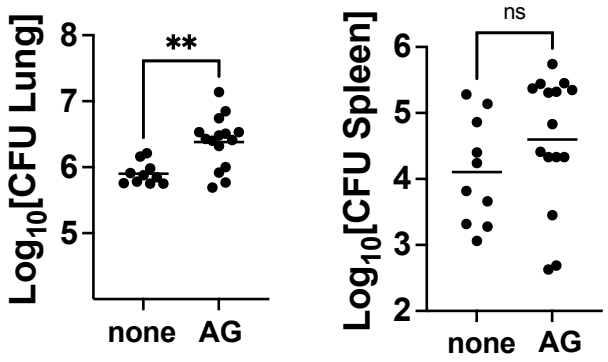

C.

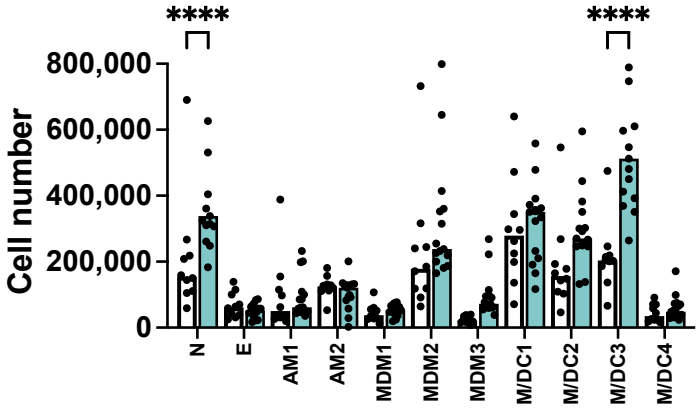

D.

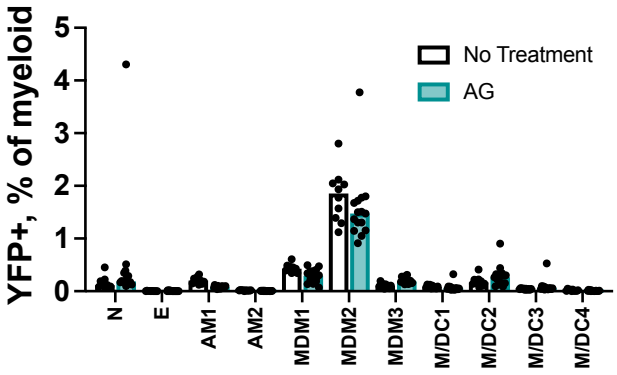

Figure 5

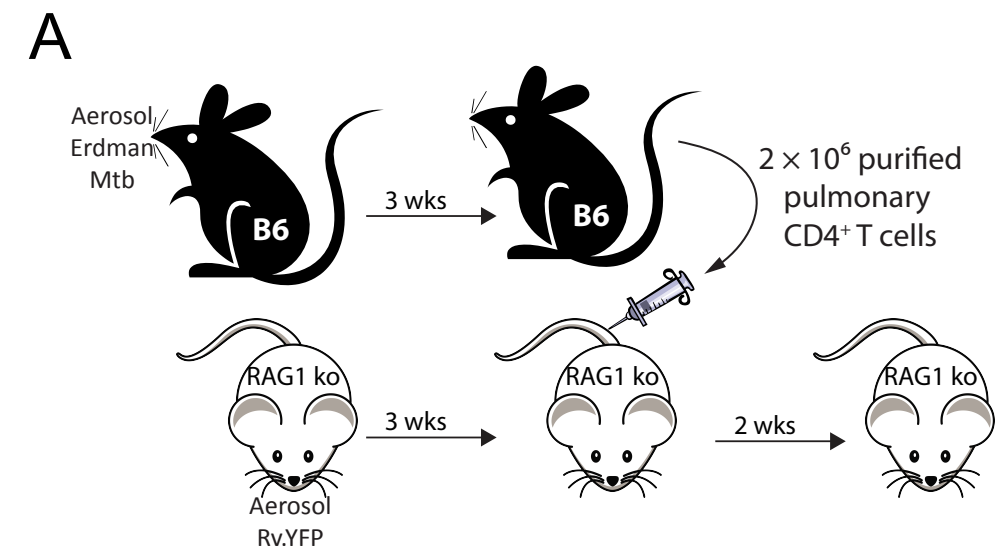

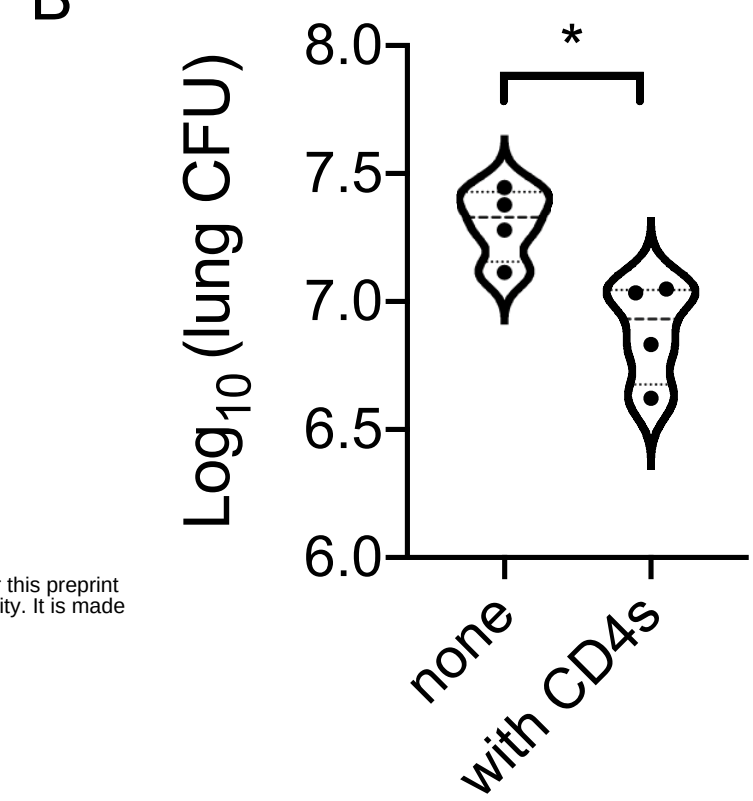

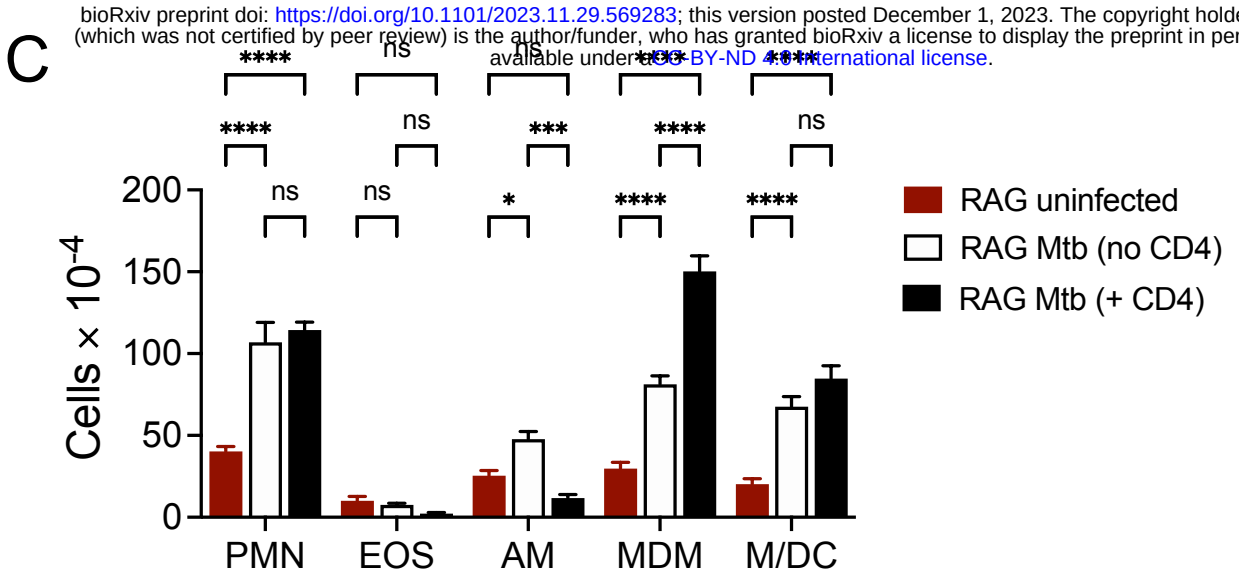

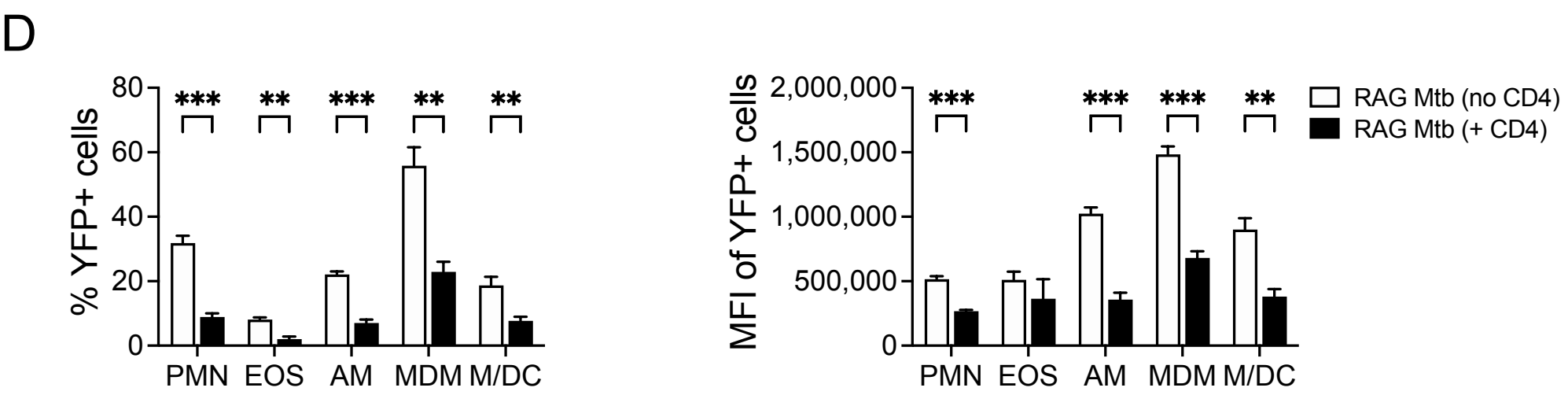

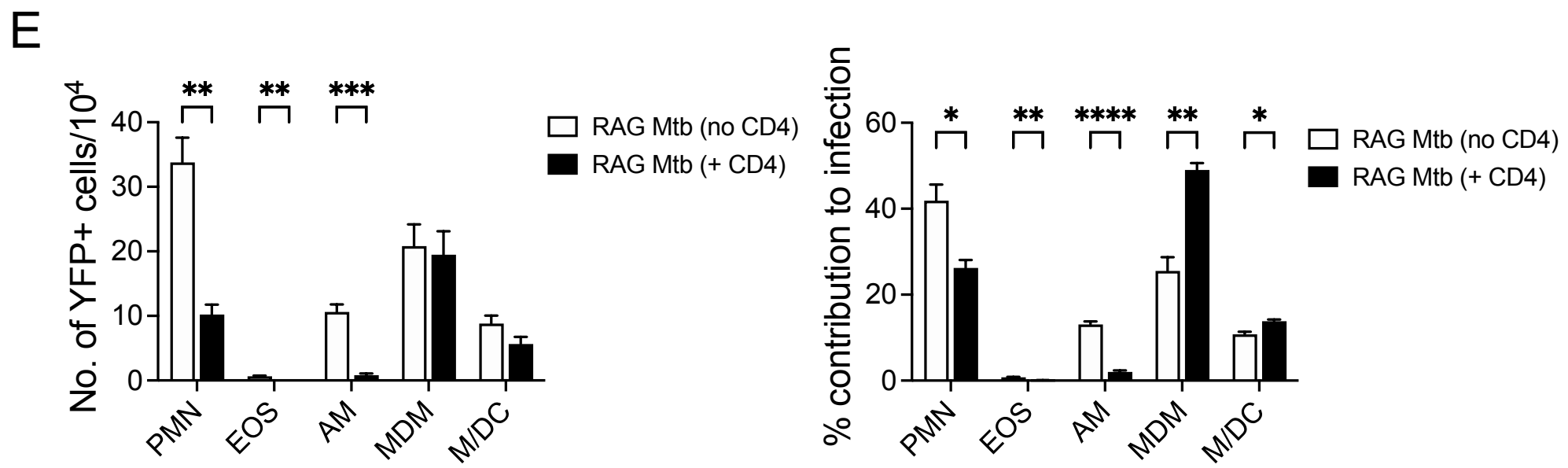

Figure 6

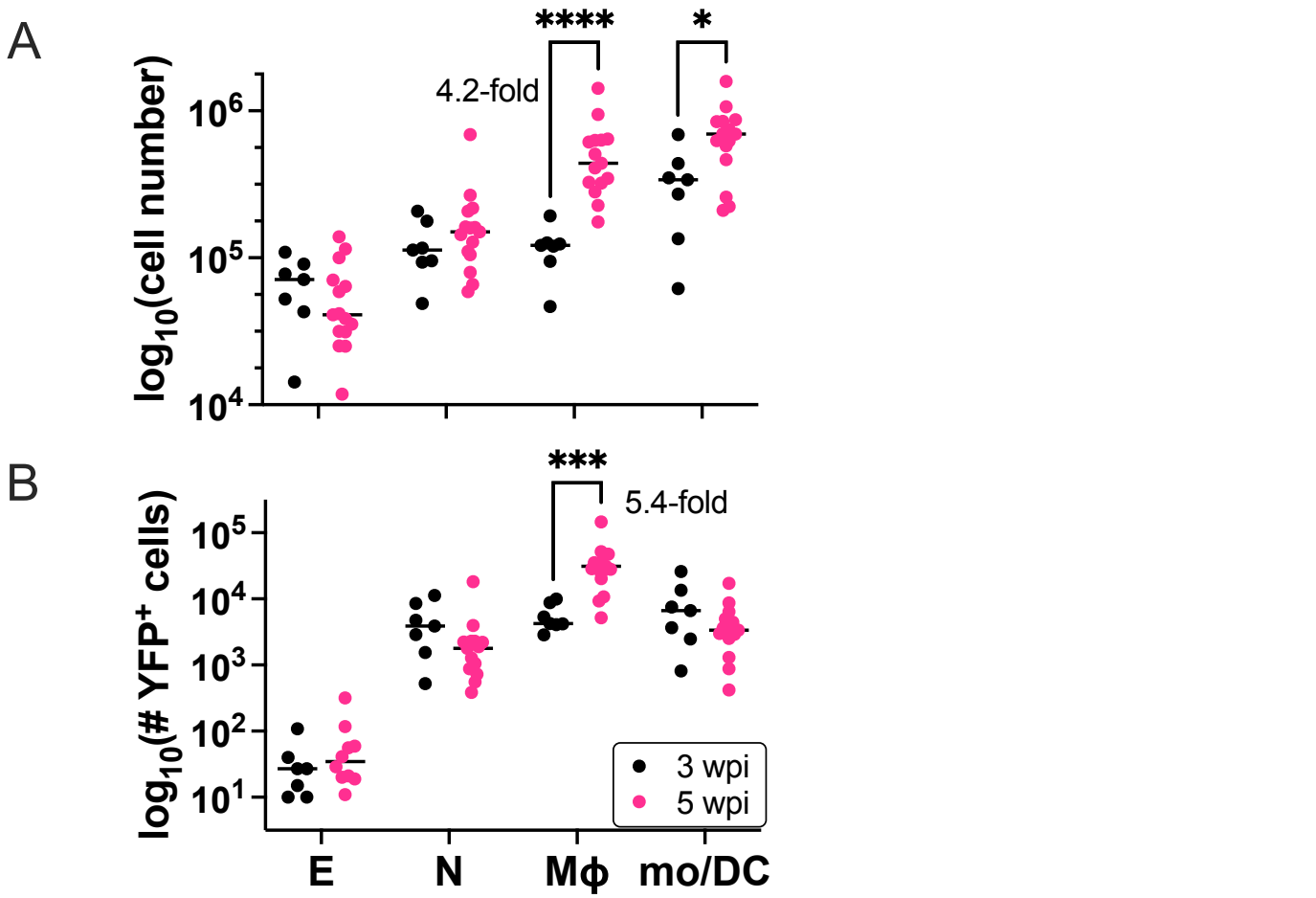

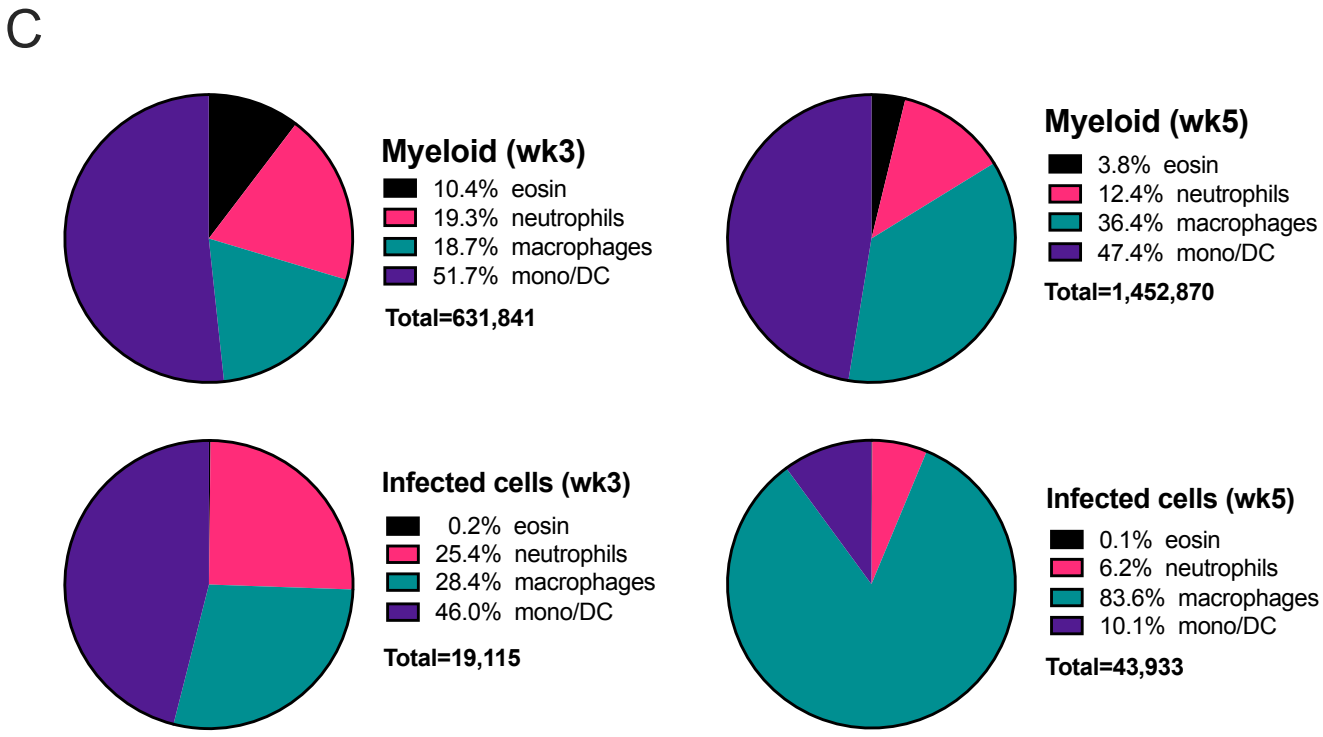

Figure S1

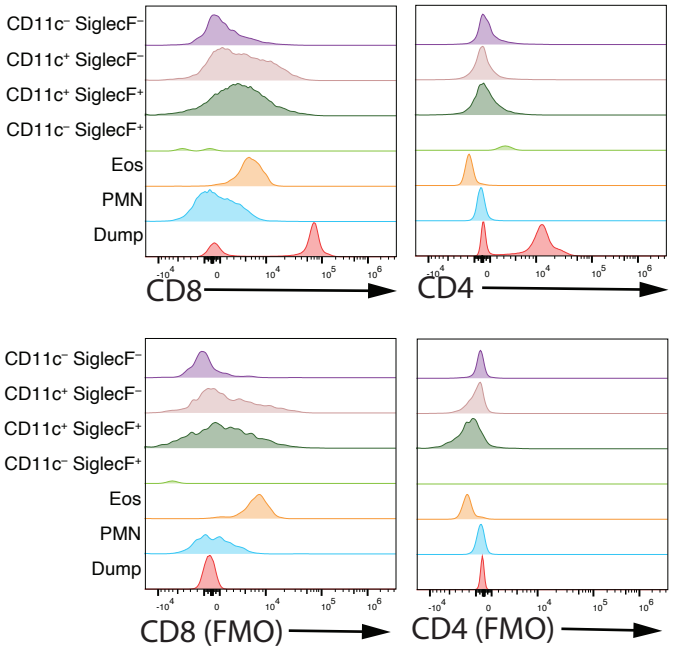

Supplemental Figure 2